Obrabotka metallov (tekhnologiya, oborudovanie, instrumenty) = Metal Working and Material Science. 2026 vol. 28 no. 2 pp. 32–48
ISSN: 1994-6309 (print) / 2541-819X (online)
DOI: 10.17212/1994-6309-2026-28.2-32-48

NSTU NETI

Obrabotka metallov -
Metal Working and Material Science

Journal homepage: http://journals.nstu.ru/obrabotka_metallov

Determination of temperature conditions of wave deformation hardening for materials synthesized by the WAAM method

Andrey Kirichek [1, a], *Dmitry Solovyev* [2, b, *], *Alexander Yashin* [2, c], *Sergey Silantyev* [2, d], *Maxim Novikov* [1, e]

[1] Bryansk State Technical University, 7 50 Let Oktyabrya Bul., Bryansk, 241035, Russian Federation
[2] Vladimir State University named after Alexander and Nikolay Stoletovs, 87 Gorkogo St., Vladimir, 600000, Russian Federation

[a] https://orcid.org/0000-0002-3823-0501, avkbgtu@gmail.com; [b] https://orcid.org/0000-0002-4475-319X, murstin@yandex.ru;
[c] https://orcid.org/0000-0002-3186-1300, yashin2102@yandex.ru; [d] https://orcid.org/0000-0002-3524-385X, ppdsio@yandex.ru;
[e] https://orcid.org/0009-0000-7552-312X, novikovmax14@yandex.ru

ARTICLE INFO

Article history:
Received: 05 February 2026
Revised: 12 February 2026
Accepted: 14 March 2026
Available online: 15 June 2026

Keywords:
Additive technologies
WAAM
Deformation hardening
Deformation wave
High temperature
Hardness

Funding
The research was carried out with the support of the Ministry of Science and Higher Education of the Russian Federation as part of basic research component of the state assignment of the Ministry of Education and Science of the Russian Federation under project No. FZWR-2024-0003 (No. 075-00150-24-03) "Development of a technological strategy and theoretical and experimental study of the key elements of the technology of additive synthesis of metal wire parts using the 3DMP method and wave thermo-deformation strengthening of synthesized machine parts."

ABSTRACT

Introduction. To reduce the number of defects and improve the mechanical properties of components fabricated by wire arc additive manufacturing (*WAAM*), the application of deformation hardening operations during the synthesis process is promising. Wave deformation hardening enables the formation of a deep hardened layer, which is particularly important for hybrid *WAAM* processes where subsequent heating of the upper layers can lead to softening of previously deposited layers. A key parameter determining the effectiveness of wave deformation hardening is the temperature at which the synthesized material is subjected to the deformation hardening. ***The purpose of this study*** is to analyze the influence of the product temperature on the efficiency of wave deformation hardening for several advanced structural materials produced by the *WAAM* method. **Methodology.** The experiment involved the synthesis of samples, followed by furnace heating to a predetermined temperature (*0.04C–19Cr–9Ni*, *0.3C–1Cr–1Mn–1Si*, *0.18C–1Cr–1Mn–1Si*, and *0.09C–1.7Cr–1Mn–0.6Mo–1Ni–0.8Ti–0.015N*: 300–900 °C; for the *97Al–3Mg* alloy: 100–500°C), after which they were subjected to hardening. To evaluate the effectiveness of the method, microhardness (*Vickers*) profiles were measured as a function of depth through the hardened layer. **Results and discussion.** The study revealed a characteristic optimal temperature range for each material within which wave deformation hardening provides the maximum strengthening effect. For austenitic steel *0.04C–19Cr–9Ni*, the greatest increase in hardness (up to 52%) was achieved when treated at 700 °C, attributed to the increased ductility of austenite and possible deformation-induced martensitic transformation; above 800 °C, recrystallization begins, reducing the effect. For medium-alloyed steels 0.3C–1Cr–1Mn–1Si, 0.18C–1Cr–1Mn–1Si, and 0.09C–1.7Cr–1Mn–0.6Mo–1Ni–0.8Ti–0.015N, the optimal range was 400–600 °C, with a maximum hardness increase of 34–50%; in this region, dynamic polygonization and carbide dispersion hardening actively occur, while recrystallization dominates at higher temperatures. For aluminum alloy *97Al–3Mg*, the effective range was 100–300 °C, with an increase in hardness of up to 24%, corresponding to the recovery condition; at 400–500 °C, the hardness drops below the initial value due to complete recrystallization. The depth of the hardened layer exceeded 3 mm for steels and reached 8 mm for the aluminum alloy, significantly greater than achieved by conventional surface plastic deformation methods. An anomalous behavior was identified for steel *0.09C–1.7Cr–1Mn–0.6Mo–1Ni–0.8Ti–0.015N*: after a decrease in hardness at 700–800 °C, an increase in hardness was observed at 900 °C, explained by secondary hardening due to the dissolution of coarse carbides and the precipitation of fine particles during cooling. The obtained data are in good agreement with known tempering and recrystallization temperatures for the materials studied. The results enabled the formulation of practical recommendations for selecting wave deformation hardening temperature conditions for integration into hybrid *WAAM* processes, depending on the material class, ensuring maximum improvement in both hardness and hardened layer depth for additively manufactured components.

For citation: Kirichek A.V., Solovyev D.L., Yashin A.V., Silantyev S.A., Novikov M.A. Determination of temperature conditions of wave deformation hardening for materials synthesized by the WAAM method. *Obrabotka metallov (tekhnologiya, oborudovanie, instrumenty) = Metal Working and Material Science*, 2026, vol. 28, no. 2, pp. 32–48. DOI: 10.17212/1994-6309-2026-28.2-32-48. (In Russian).

*** Corresponding author**
Solovyev Dmitry L., D.Sc. (Engineering), Professor
Vladimir State University named after Alexander and Nikolay Stoletovs,
87 Gorkogo St.,
600000, Vladimir, Russian Federation
Tel.: +7 920 900-46-42, **e-mail:** murstin@yandex.ru

Introduction

The development of metal additive manufacturing presents new challenges for mechanical engineering, particularly regarding the need to ensure the required mechanical properties of manufactured products [1–4]. Among the most promising methods for producing medium- and large-sized metal parts with complex geometry is wire arc additive manufacturing (*WAAM*) [5, 6]. This technique, based on layer-by-layer deposition of metal wire using an electric arc, offers high productivity, cost efficiency, and the ability to process a wide range of structural materials [7–9]. However, like many other additive processes, *WAAM* is characterized by non-uniform mechanical properties throughout the component volume and the presence of residual stresses, which together can limit the application of such parts in critical structures subjected to cyclic and impact loads [10–12].

To expand the functionality of *WAAM*-based additive manufacturing, hybrid approaches are being actively developed. These combine additive synthesis with strengthening, which can be performed either as post-process heat treatment [13] or as mechanical deformation at various stages – both after manufacturing and during deposition [14–18]. The effectiveness of deformation hardening applied during synthesis depends directly on the depth of the strengthened layer, since subsequent heating of the upper deposited layers during additive manufacturing leads to their thermal softening. Consequently, to maintain high mechanical properties in the finished product, the material located outside the recrystallization zone formed during repeated heating must be strengthened.

Various deformation hardening methods have been employed in hybrid *WAAM* processes. For instance, interlayer rolling of *WAAM*-produced *Ti–6Al–4V* resulted in grain refinement and a transition from a columnar to an equiaxed microstructure, accompanied by increased strength [19]. Rolling during synthesis of the same alloy under loads of 60 and 90 kN enabled structure refinement to a depth of 3 mm from the surface [17], while for *Al-6.3Cu* alloy, the effect was enhanced by subsequent *T6* heat treatment [20]. Impact minting with a pneumatic hammer (180 Hz, 6 bar, Ø4 mm) for *Ti–6Al–4V* also ensures structure refinement to a depth of 3 mm, formation of compressive residual stresses, and an increase in hardness from 420 to 492 HV [18]. Laser impact hardening can refine grain size – for example, by 22 % for *2319* aluminum alloy – and increase hardness; however, the affected zone is limited to a surface layer of less than 1 mm [21].

A drawback of the methods discussed is the increased cycle time due to the need to cool each layer, which reduces *WAAM* productivity. Furthermore, the hardened zone depth is limited to 1–3 mm, which often does not extend beyond the recrystallization zone.

An important parameter governing the effectiveness of deformation hardening, particularly for *WAAM*-synthesized materials, is the temperature at which deformation occurs. On one hand, preheating may be necessary to reduce deformation resistance and prevent cracking – an approach typical of thermomechanical processing. On the other hand, in hybrid additive processes, deformation hardening may be applied to hot, freshly deposited metal, making temperature not a controllable parameter but rather a consequence of the process that requires careful investigation.

This is illustrated by examples of deformation hardening of preheated metallic materials [22]. Shot peening of a titanium alloy heated to 280 °C made it possible to increase the hardening depth from 100 μm to 160 μm compared to shot peening at room temperature [23]. During shot peening of spring steels, maximum hardness was achieved at a preheating temperature of 200 °C, with further heating leading to a hardness decrease due to excessive softening [24]. For laser impact treatment of *A356* aluminum alloy, raising the operating temperature from room temperature to 180° C increased the maximum hardness from 110 to 180 HV and the hardened layer depth from 0.55 to 0.9 mm [25].

Examples of deformation hardening of heated metal during *WAAM* deposition have also been reported. Increasing the operating temperature from room temperature to 300 °C enabled an increase in the surface hardness of synthesized *Ti64* alloy blanks from 3.90 to 4.25 GPa [26]. A similar trend was observed for *Inconel 690* nickel alloy, where the optimal heating temperature (300 °C) during ultrasonic treatment promoted increases in both hardness and hardened layer depth, but exceeding 700 °C led to a hardness decrease [27]. Pneumatic minting of uncooled *WAAM 95Al-5Mg* alloy (energy 7.1 J, frequency 3,200 bpm) increased strength and ductility by 15–20%; however, the temperature conditions responsible for this effect were not detailed [28]. In the *HF-WAAM* method for *AISI 316L* steel, hot minting at 900 °C with forces of 17–55 N also resulted in increased strength and reduced porosity, but the high temperature promoted grain growth and phase composition changes [15].

Based on the above analysis, it can be concluded that hybrid *WAAM* technologies are needed that combine deep deformation hardening (greater than 3 mm) with the ability to process uncooled material directly within the *WAAM* cycle, while maintaining the temperature within a strictly defined range that prevents softening and undesirable recrystallization.

In this context, wave deformation hardening (*WDH*), which can be integrated directly into the deposition process, appears highly promising. *WDH* involves surface treatment with controlled impact pulses whose energy and shape are governed by the geometry of the impact system, comprising a striker and a waveguide. During hardening, the striker impacts the waveguide, which is statically pressed against the component through a tool. This generates plane acoustic waves in the impact system, which are transformed into impact pulses of the desired shape at the contact area. By selecting the optimal pulse shape for a given material and processing conditions, maximum impact energy transfer is achieved, thereby increasing process efficiency and ensuring the formation of a deep hardened layer (up to 6–8 mm) [29].

When integrating *WDH* into *WAAM*-based material synthesis, determining an optimal temperature range for *WDH* is of great importance. On one hand, the temperature should maximize the strengthening effect through grain refinement, twinning, and slip line formation. On the other hand, it should prevent recrystallization processes that would negate the work hardening effect.

The objective of this study is to analyze the effect of preheating temperature on the effectiveness of wave deformation hardening for a range of promising structural materials produced by *WAAM*. Effectiveness is assessed based on the degree of surface layer hardening.

To achieve this objective, ***the following tasks*** were performed:

– to experimentally determine the surface layer hardness as a function of heating temperature for samples without subsequent *WDH* and for samples after *WDH*;

– to establish optimal temperature ranges for *WDH* that ensure maximum hardness and hardened layer depth;

– to conduct a comparative analysis of the behavior of different material classes (austenitic and medium-alloy steels, aluminum alloy) during *WDH* and to formulate conclusions.

Research methodology

The materials selected for the study included:

– *0.09C–1.7Cr–1Mn–0.6Mo–1Ni–0.8T–0.015N* alloy steel,

– *0.3C–1Cr–1Mn–1Si* medium-alloy structural steel,

– *0.18C–1Cr–1Mn–1Si* low-carbon medium-alloy steel,

– *0.04C–19Cr–9Ni* austenitic stainless steel,

– *97Al–3Mg* aluminum wrought alloy.

These materials cover a wide range of applications, from critical welded structures (*0.09C–1.7Cr–1Mn–0.6Mo–1Ni–0.8T–0.015N* steel) to components operating in aggressive environments (*0.04C–19Cr–9Ni* steel).

Experimental algorithm:

– three-layer deposition of a specimen (specimen size: 90 × 120 mm; the height of each synthesized layer was 2.2 mm for steels and 2.5 mm for the *97Al–3Mg* aluminum alloy);

– heating the specimen to the required temperature in a furnace and holding for at least 30 minutes;

– wave deformation hardening (*WDH*) – the feed direction is perpendicular to the deposition feed direction (Fig. 1); after *WDH*, the specimens are cooled in air;

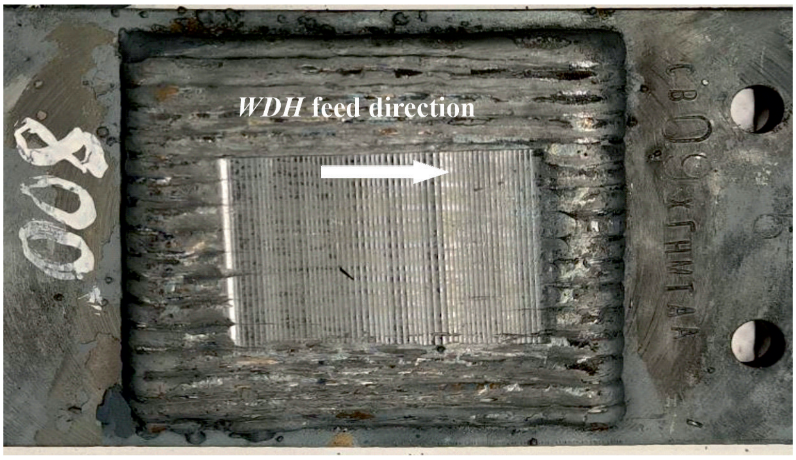

Fig. 1. Sample of *0.09C–1.7Cr–1Mn–0.6Mo–1Ni–0.8Ti–0.015N* steel after wave deformation hardening (*WDH*) at 800 °C

– cutting the obtained specimens in the longitudinal and transverse directions relative to the *WDH* feed direction and preparing microsections along the depth of the surface layer; specimens are cut out for hardness measurements beneath the hardened and non-hardened surfaces;

– *Vickers* hardness measurement – performed at room temperature (at least three tracks along the depth of the surface layer with a step of 0.3 mm) in each *WDH* feed direction;

– for each depth level (comprising at least three measurement points in two feed directions), the average hardness value was calculated at that depth level (Fig. 2); for each sample, the average hardness was also determined from all measured values.

The standard deviation of the measured hardness values did not exceed 10%, indicating good reproducibility of the results.

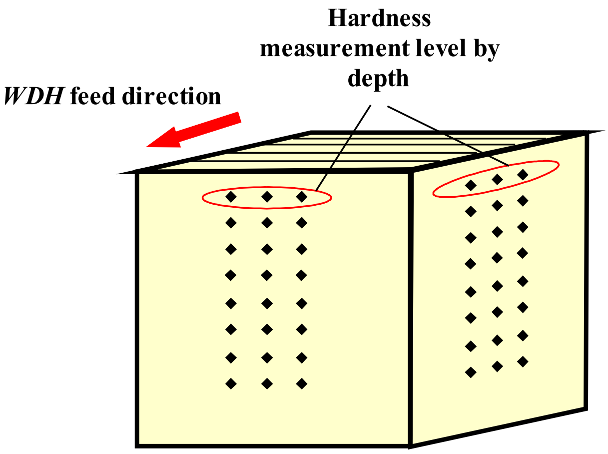

Fig. 2. Schematic of the hardness measurement procedure

Hardness measurements of synthesized samples after heating without subsequent hardening and cooling, and of samples after heating followed by *WDH* and cooling, enable the determination of not only the effective temperature for *WDH* but also the possible influence of heat treatment (heating followed by air cooling) after synthesis.

To evaluate the effectiveness of *WDH*, the degree of hardening was used:

$$\Delta HV = \frac{HV_0 - HV}{HV} 100\%,$$

where HV_0 and *HV* are the average hardness values at a given depth level, respectively, after heating without subsequent *WDH* and cooling, and after heating with subsequent *WDH* and cooling.

When determining the synthesis conditions, the primary objective was to obtain high-quality samples with a minimum number of pores (Table 1).

When selecting the heating temperature of synthesized materials for experimental studies, it is necessary to rely on their characteristics obtained during heat treatment.

It is known that forging of *0.3C-1Cr-1Mn-1Si* steel begins at 1,240 °C and ends at 800 °C. To improve mechanical properties, parts made of *0.3C-1Cr-1Mn-1Si* steel are subjected to quenching and tempering. Quenching is recommended at 880 °C, with cooling in oil, which eliminates the possibility of surface and structural deformations. Quenching involves restructuring the crystal lattice. This process

Table 1

Synthesis parameters (*WAAM* deposition conditions)

Parameter	Material				
	0.04*C*–19*Cr*–9*Ni*	0.3C–1*Cr*–1*Mn*–1*Si*	0.18C–1*Cr*–1*Mn*–1*Si*	0.09C–1.7*Cr*–1*Mn*–0.6*Mo*–1*Ni*–0.8*Ti*–0.015*N*	97*Al*–3*Mg*
Current (A)	170	140	150	145	125
Voltage (V)	18.3	23.9	18.9	17.3	18.7
Wire feed rate (m/min)	6.37	4.9	4.8	5	7.3
Feedstock feed rate (mm/min)	1000	1000	1000	1000	1000
Wire diameter (mm)	1.2	1.2	1.2	1.2	1.2

causes internal stresses, which subsequently lead to structural cracks. Tempering at 540–550 °C solves this problem. Furthermore, the martensite formed during quenching transforms into sorbite, resulting in a homogeneous and fine-grained metal structure. The low heating temperature makes it possible to use water as a cooling medium. In addition, conducted studies on the combined hardening process (*WDH* + heat treatment: quenching + tempering) for *0.3C-1Cr-1Mn-1Si* steel showed that the best results are achieved with tempering at 550 °C (the range of tempering temperatures studied was 200–600 °C) [30]. Therefore, it can be assumed that for *0.3C-1Cr-1Mn-1Si* steel, the sample temperature for *WDH* at which the greatest hardness will be achieved lies in the range of 500–600°C.

97Al–3Mg aluminum alloy undergoes hot deformation in the temperature range of 430 °C down to 320 °C without thermal strengthening. To relieve internal stress, low-temperature annealing is performed at temperatures of 250–300 °C, and high-temperature annealing at 350–420 °C. Therefore, it can be assumed that for *97Al–3Mg* alloy, the sample temperature for *WDH* at which the greatest hardness is achieved lies in the range of 250–350 °C.

Products made from the other materials under study are produced only by synthesis, so there is no data related to the effect of heat treatment on their mechanical properties. However, it should be noted that recrystallization annealing after work hardening for most steels occurs at a heating temperature of 0.4–0.6 of the melting temperature, i.e. in the temperature range of 600–700 °C.

Therefore, the following heating temperatures before *WDH* were selected for the studies:

– for steels: 300, 400, 500, 600, 700, 800, 900 °C;

– for the aluminum alloy: 100, 200, 300, 400, 500 °C.

WDH of the synthesized samples was carried out with an impact energy of 150 J and a frequency of 9 Hz. A cylindrical roller with a diameter of 10 mm and a length of 40 mm was used as the tool. The feed rate was selected based on the condition of ensuring an overlap coefficient of prints of 0.45, at which a sufficiently strengthened structure is formed and the possibility of overworking is excluded [31].

Results and their discussion

Based on the experimental data obtained for *0.04C–19Cr–9Ni* steel, it was found that, depending on the heating temperature of samples without *WDH*, the average hardness follows a parabolic trend, with a minimum of 254 HV at 600 °C and maxima of 275 HV at 300 °C and 800 °C (Fig. 3). This is consistent with the findings reported in [32], where it was noted that samples with a *0.04C–19Cr–9Ni* coating retain their hardness when heated to 600 °C.

For samples subjected to *WDH*, the average surface layer hardness increases with temperature, reaching a maximum of 335 HV at 700 °C, where the maximum degree of hardening reached 52 % (Fig. 4). Further heating leads to a decrease in the hardness of the hardened metal. This reduction in *WDH* effectiveness at temperatures above 700 °C corresponds to the results of [33], where annealing of cold-formed *AISI 304* steel at 800 °C also caused a sharp drop in hardness due to the onset of recrystallization.

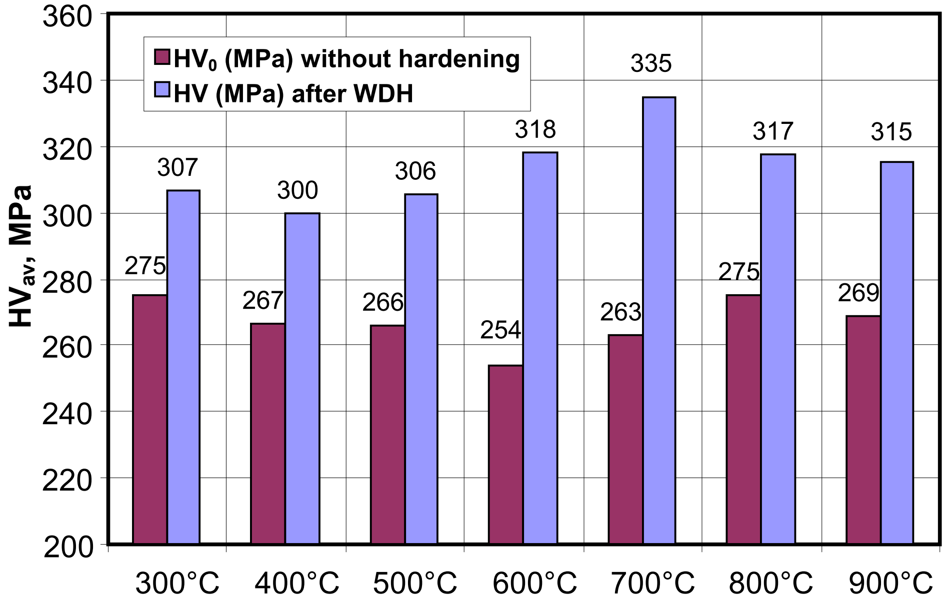

Fig. 3. Change in average hardness of the surface layer without hardening and after wave deformation hardening (*WDH*) at different temperatures for the synthesized 0.04*C*–19*Cr*–9*Ni* steel sample

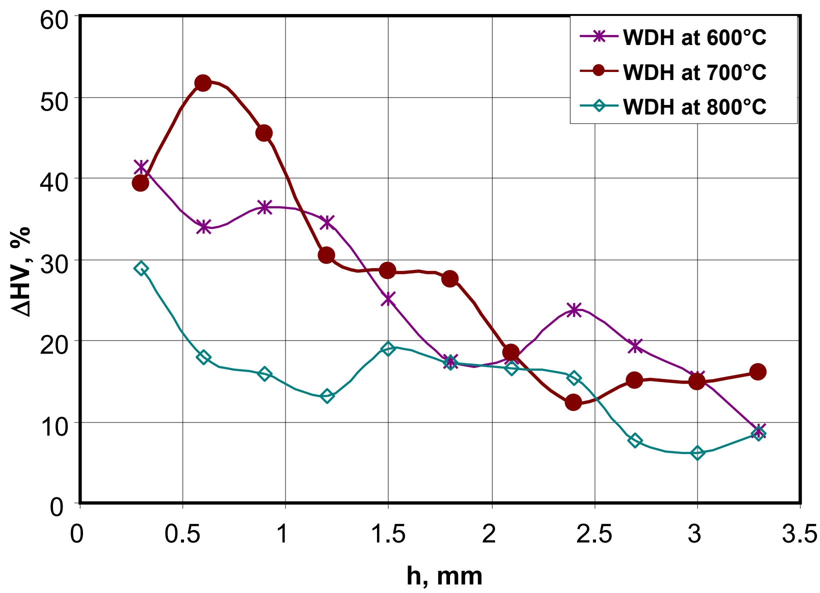

Fig. 4. Change in the degree of hardening as a function of depth through the surface layer after wave deformation hardening (*WDH*) at different temperatures for the synthesized 0.04*C*–19*Cr*–9*Ni* steel sample

For *0.3C–1Cr–1Mn–1Si* steel, it was found that when heating samples without *WDH* from 300 °C to 400 °C, the average hardness increased from 239 HV to 253 HV, then decreased with further temperature rise, reaching 200 HV at 800–900 °C (Fig. 5). For samples after *WDH*, the surface layer hardness increased with temperature, reaching a maximum at 500 °C with an average hardness of 291 HV and a maximum hardening degree of 34% (Fig. 6). Further heating led to a decrease in the hardness of the hardened metal, and at 900 °C, the hardness of the hardened samples became lower than that of the unhardened metal. This observed behavior is confirmed by the results of [34], according to which deformation of 0.3C–1Cr–1Mn–1Si steel at temperatures of 800–1,000 °C is accompanied by softening due to recovery and dynamic recrystallization.

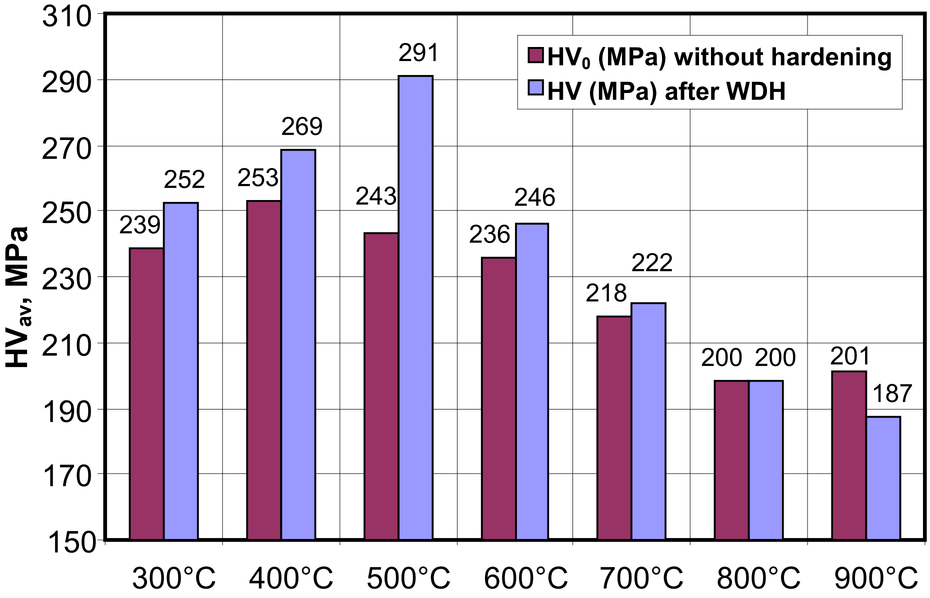

Fig. 5. Change in average hardness of the surface layer without hardening and after wave deformation hardening (*WDH*) at different temperatures for the synthesized 0.3C–1*Cr*–1*Mn*–1*Si* steel sample

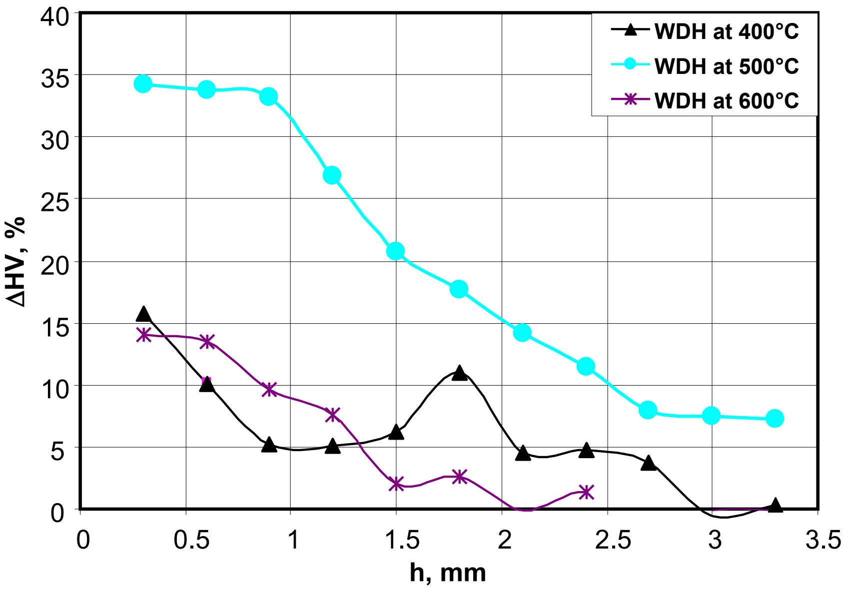

Fig. 6. Change in the degree of hardening as a function of depth through the surface layer after wave deformation hardening (*WDH*) at different temperatures for the synthesized 0.3C–1*Cr*–1*Mn*–1*Si* steel sample

For *0.18C–1Cr–1Mn–1Si* steel, it was found that when heating samples without *WDH*, the maximum average hardness (197 HV) was obtained at 300 °C. With increasing temperature, the average hardness gradually dropped to 162 HV at 800–900 °C (Fig. 7). For samples subjected to *WDH*, in the temperature range of 300–500 °C, the average hardness reached a maximum of 233–240 HV, with a maximum hardening degree of 50% (Fig. 8). Further heating led to a decrease in the hardness of the hardened metal, and at a sample temperature of 900 °C, the average hardness was 175 HV. The observed presence of a temperature range in which *WDH* is effective, followed by softening upon overheating, is consistent with the conclusions of [35], which studied the deformability of *0.18C–1Cr–1Mn–1Si* steel.

For *0.09C–1.7Cr–1Mn-0.6Mo–1Ni–0.8T–0.015N* steel, it was found that when heating samples to 600 °C without *WDH*, the average hardness remained virtually unchanged (263–269 HV). With increasing

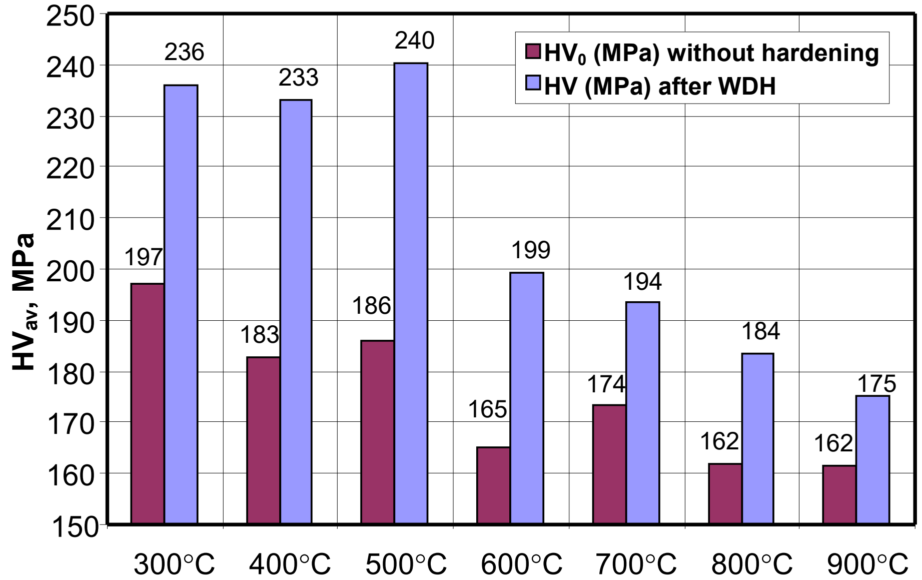

Fig. 7. Change in average hardness of the surface layer without hardening and after wave deformation hardening (*WDH*) at different temperatures for the synthesized 0.18C-1*Cr*-1*Mn*-1*Si* steel sample

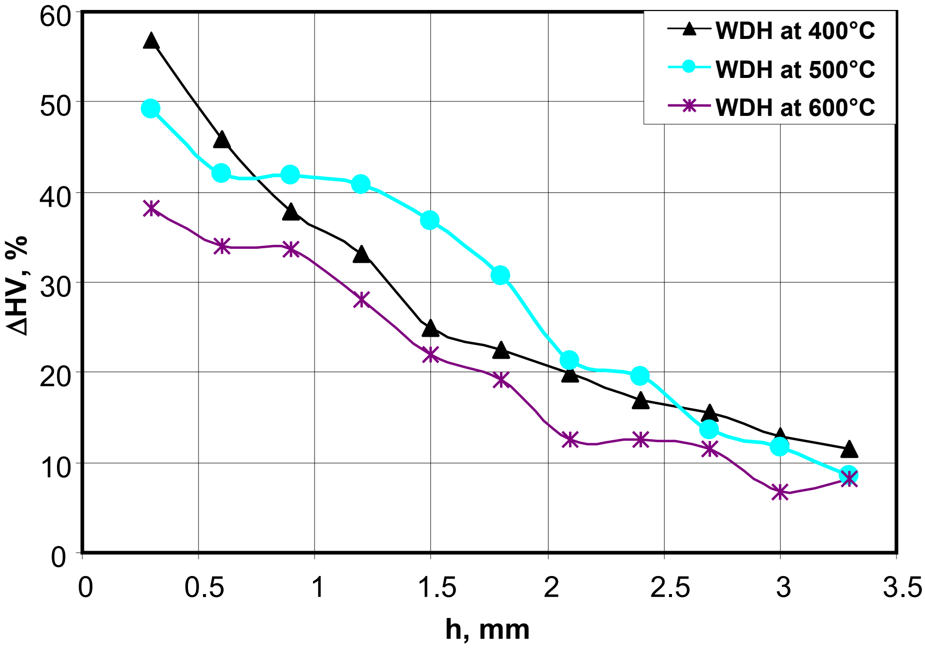

Fig. 8. Change in the degree of hardening as a function of depth through the surface layer after wave deformation hardening (*WDH*) at different temperatures for the synthesized 0.18C–1*Cr*–1*Mn*–1*Si* steel sample

temperature, the average hardness dropped to 222 HV at 700 °C, then to 206 HV at 800 °C, after which it increased to 242 HV at 900 °C (Fig. 9). For samples subjected to *WDH*, as well as for those without hardening, in the temperature range of 300–600 °C, the maximum average hardness was established and amounted to 284–289 HV, with a maximum hardening degree of 35% (Fig. 10). Further heating also led to a sharp decrease in the hardness of the hardened metal to 221–230 HV at 700–800 °C, followed by an increase to 252 HV at a sample temperature of 900 °C. The observed repeated increase in hardness at 900 °C may be associated with the phenomenon of secondary hardness, which is characteristic of alloy steels containing carbide-forming elements (Mo, Cr, V, Ti), and is caused by the dissolution of large carbides followed by the precipitation of dispersed particles upon cooling [36].

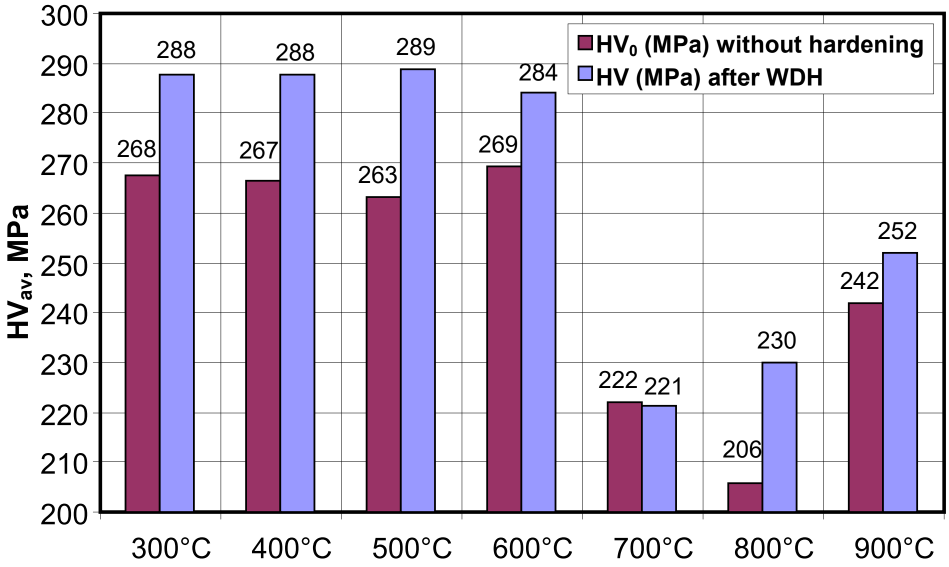

Fig. 9. Change in average hardness of the surface layer without hardening and after wave deformation hardening (*WDH*) at different temperatures for the synthesized 0.09C–1.7*Cr*–1*Mn*–0.6*Mo*–1*Ni*–0.8*Ti*–0.015*N* steel sample

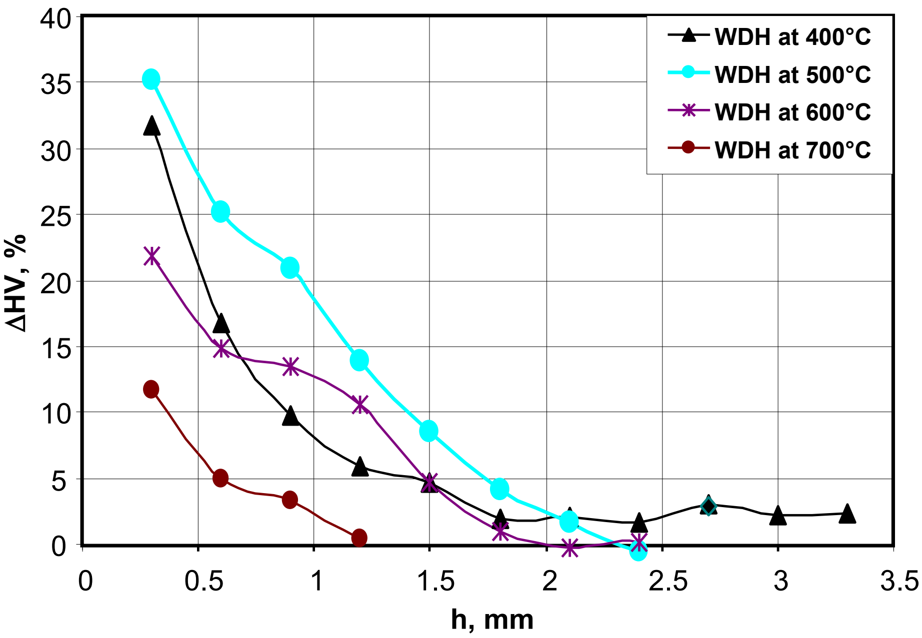

Fig. 10. Change in the degree of hardening as a function of depth through the surface layer after wave deformation hardening (*WDH*) at different temperatures for the synthesized 0.09C-1.7*Cr-1Mn–0.6Mo–1Ni–0.8Ti–0.015N* steel sample

For *97Al–3Mg* aluminum alloy, it was found that when heating samples without *WDH*, the average hardness remained virtually unchanged (74–77 HV) over the entire test temperature range of 100–500 °C (Fig. 11). For samples subjected to *WDH*, in the temperature range of 100–300 °C, the average hardness reached a maximum of 83–88 HV, with a maximum hardening degree of 24% (Fig. 12). Further heating led to a decrease in the hardness of the hardened metal, and at a sample temperature of 500 °C, the hardness became lower than that of the unhardened material. These data are consistent with the known temperature threshold of 300 °C, above which recrystallization is activated, neutralizing the work hardening effect [37].

The obtained results can be explained as follows. In the optimal temperature range, the material retains sufficient ductility for deformation, while softening processes remain slow. During *WDH*, a high density

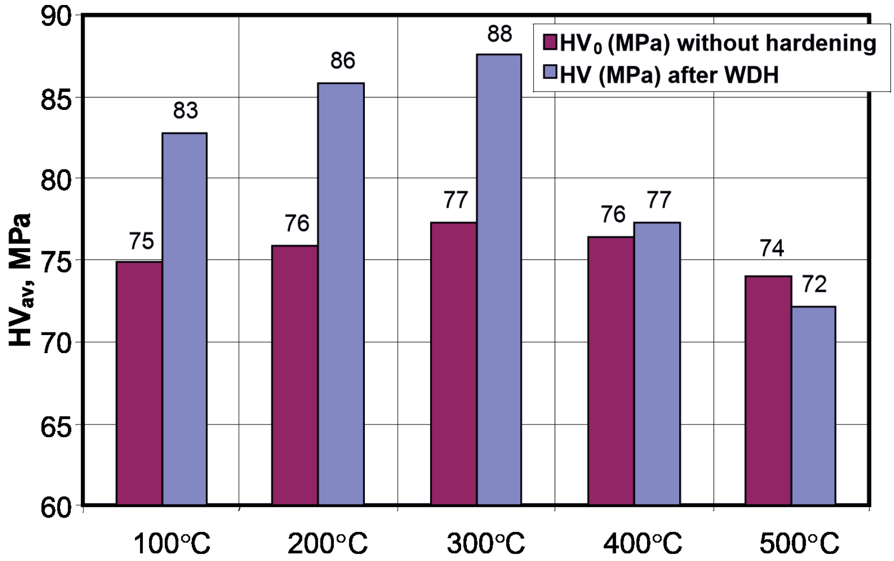

Fig. 11. Change in average hardness of the surface layer without hardening and after wave deformation hardening (*WDH*) at different temperatures for the synthesized *97Al–3Mg* aluminum alloy

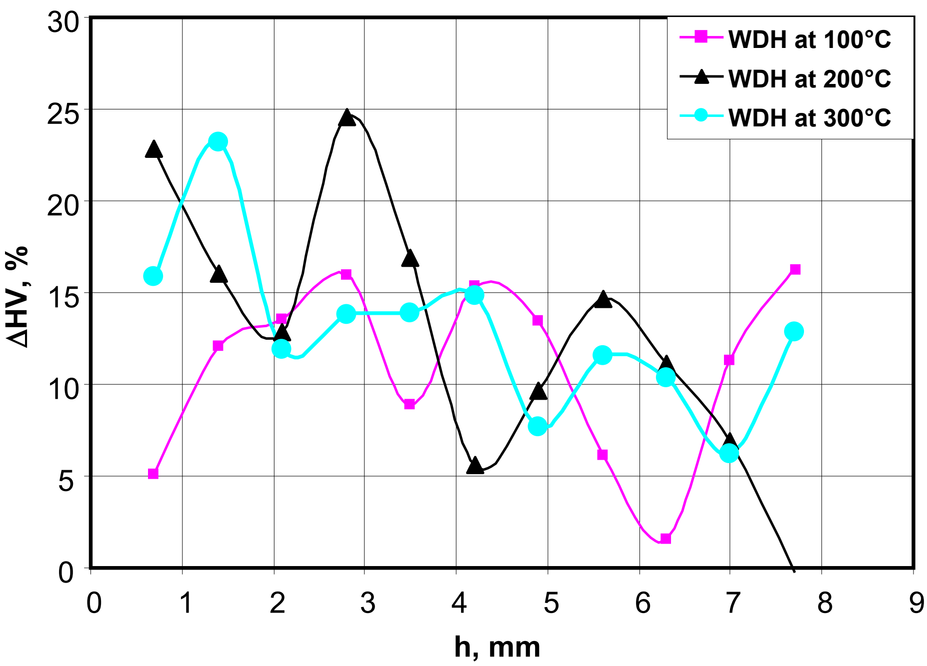

Fig. 12. Change in the degree of hardening as a function of depth through the surface layer after wave deformation hardening (*WDH*) at different temperatures for the synthesized *97Al–3Mg* aluminum alloy

of dislocations is generated in the material, leading to their chaotic distribution. At a sufficient degree of deformation, a cellular and fragmented substructure is formed. Mechanical twinning and the formation of slip bands may also contribute to strengthening. The decrease in hardness after *WDH* at high temperatures is likely due to the activation of recrystallization processes. High temperature provides sufficient energy for the climb and annihilation of dislocations accumulated during *WDH*. Additionally, dispersed precipitates of carbides and nitrides, which act as barriers to dislocation motion, may dissolve.

0.04C-19Cr-9Ni steel is austenitic and does not undergo phase transformations upon heating and cooling. However, during deformation in the range of 300–500 °C, martensite formation is possible, which can provide an additional contribution to strengthening [38]. At 700 °C, martensitic phases are unstable, and strengthening is ensured solely by dislocation mechanisms. At temperatures above 800 °C, primary recrystallization begins, forming new equiaxed grains, which leads to a sharp drop in hardness.

When heated to 500 °C, *0.3C–1Cr–1Mn–1Si* steel develops a ferrite-cementite structure (tempered sorbite). Deformation under these conditions promotes additional precipitation strengthening due to the precipitation of carbides from supersaturated ferrite. *0.18C–1Cr–1Mn–1Si* steel behaves similarly, but its lower carbon content reduces the potential for carbide strengthening, which is offset by a more significant contribution from deformation hardening (hardening degree of up to 50%).

0.09C–1.7Cr–1Mn-0.6Mo–1Ni–0.8T–-0.015N steel is distinguished by the presence of strong carbide-forming elements (Mo, Cr, V, Ti). This explains its anomalous behavior at 900 °C: after a drop in hardness in the 700–800 °C range (carbide coagulation, recrystallization), heating to 900 °C causes the dissolution of large carbides and enrichment of austenite with alloying elements. Upon subsequent air cooling, dispersed carbides (secondary hardness) may precipitate from this austenite, or bainitic-martensitic structures may form, resulting in a repeated increase in hardness to 242 HV (Fig. 9).

97Al–3Mg aluminum alloy is classified as a non-heat-hardenable alloy. Its primary strengthening mechanism is the accumulation of dislocations and the formation of a cellular substructure. The recommended deformation hardening temperature range of 100–300 °C corresponds to the region where the diffusion mobility of Mg atoms is still low and recovery is slow. Intense recrystallization is initiated at temperatures above 300 °C. Heating to 500 °C (≈0.5 times the absolute melting point) completes recrystallization, and the hardness drops below the initial value.

For *0.3C–1Cr–1Mn–1Si* steel and *97Al–3Mg* alloy, the experimentally obtained temperature window effective for *WDH* confirms previously stated assumptions.

The *WDH* results for all studied materials are summarized in Table 2.

Table 2

WDH results for the materials under study

Material	Optimal *WDH* temperature range, °C	Max. average hardness after *WDH*, HV_{av}	Max. hardening degree, Δ*HV*, %	Main features
0.04*C*-19*Cr*-9*Ni*	~700 °C	335	52 %	Greatest hardness increase. Without *WDH*, minimum hardness occurs at 600 °C (tempering). Peak *WDH* effectiveness coincides with increased austenite ductility, facilitating deformation hardening
0.3C-1*Cr*-1*Mn*-1*Si*	~500 °C	291	34 %	Sharp decline in *WDH* effectiveness above 500 °C. At 900 °C, hardness after *WDH* is lower than without *WDH*, indicating complete recrystallization
0.18C-1*Cr*-1*Mn*-1*Si*	300–500 °C	233–240	50 %	Wide optimal temperature range. High hardening degree. Without *WDH*, gradual hardness decrease with increasing temperature (tempering).
0.09C-1.7*Cr*-1*Mn*-0.6*Mo*-1*Ni*-0.8*Ti*-0.015*N*	300–600 °C	284–289	35 %	Most stable hardness without *WDH* in the 300–600 °C range. Sharp drop in *WDH* effectiveness at 700–800 °C, followed by partial recovery at 900 °C, possibly due to secondary hardening
97*Al*-3*Mg*	100–300 °C	83–88	24 %	Smallest absolute hardness increase, typical for aluminum-based alloys. *WDH* ineffective at 500 °C. Optimal temperatures significantly lower than for steels due to low recrystallization temperature of aluminum alloys

Analysis of the depth-wise hardening degree distribution diagrams reveals that, under the recommended temperature conditions, the hardened layer depth exceeds 3 mm for steels and reaches 8 mm for the aluminum alloy.

Conclusions

Preheating without subsequent deformation affects the hardness of different materials in various ways: from a parabolic dependence (*0.04C–19Cr–9Ni*) to a monotonic decrease (*0.18C–1Cr–1Mn–1Si*) or hardness retention over a wide range (*0.09C–1.7Cr–1Mn-0.6Mo–1Ni–0.8T–-0.015N*, *97Al–3Mg*). This is due to differences in phase transformations and tempering behavior.

WDH is a highly effective method for locally increasing the hardness (by 24–52%) of the surface layer of *WAAM*-synthesized steel and aluminum alloy parts. The hardened layer depth exceeds 3 mm for steels and 8 mm for aluminum alloy. Each material has a specific temperature range within which *WDH* provides the maximum hardening effect. Exceeding this range (at either low or high temperatures) significantly reduces the effectiveness of the process.

An upper temperature limit was identified (700–900 °C for steels and 350–400 °C for aluminum alloy), above which the hardness of the sample after *WDH* decreases to the level of, or even below, that of the sample without *WDH*. This is due to the activation of recrystallization processes, which neutralize the deformation hardening effect. Austenitic *0.04C–19Cr–9Ni* stainless steel is characterized by the highest relative increase in hardness (up to 52%) at the highest optimal temperature (700 °C). Low- and medium-alloy steels (*0.3C–1Cr–1Mn–1Si*, *0.18C–1Cr–1Mn–1Si*, and 0.09C–1.7Cr–1Mn–0.6Mo–1Ni–0.8T–0.015N) exhibit similar recommended temperature ranges for deformation hardening (400–600 °C), but differ in the absolute hardness increase (34–50%). The highest degree of hardening (50%) was achieved for *0.18C–1Cr–1Mn–1Si* steel, and the lowest (34%) for *0.3C–1Cr–1Mn–1Si*.

The *97Al–3Mg* aluminum alloy has a significantly lower recommended temperature range (100–300 °C) and a low degree of hardening (24%), which is due to the low recrystallization temperature of aluminum alloys and a different strengthening mechanism (dislocation accumulation and formation of a cellular substructure).

When integrating *WDH* into a hybrid *WAAM* process for materials with well-studied heat treatment modes (using *0.3C–1Cr–1Mn–1Si* steel and *97Al–3Mg* alloy as examples), a correlation is observed between the recommended temperature ranges for *WDH* and the temperatures used for heat treatment. This suggests that known heat treatment data can serve as a preliminary guide when selecting temperature conditions for *WDH*. For materials used solely for synthesis, preliminary testing (similar to that presented in this study) is necessary to accurately determine the individual optimal temperature window, which will maximize the strengthening effect and ensure the stability of the resulting product's properties.

These results can be used not only for additive manufacturing but also for thermomechanical strengthening, where metal is preheated to improve plastic deformation conditions.

References

1. Vafadar A., Guzzomi F., Rassau A., Hayward K. Advances in metal additive manufacturing: A review of common processes, industrial applications, and current challenges. *Applied Sciences*, 2021, vol. 11 (3), p. 1213. DOI: 10.3390/app11031213.

2. Sames W.J., List F.A., Pannala S., Dehoff R.R., Babu S.S. The metallurgy and processing science of metal additive manufacturing. *International Materials Reviews*, 2016, vol. 61 (5), pp. 315–360. DOI: 10.1080/09506608.2015.1116649.

3. Ding D., Pan Z., Cuiuri D., Li H. Wire-feed additive manufacturing of metal components: technologies, developments and future interests. *The International Journal of Advanced Manufacturing Technology*, 2015, vol. 81 (1–4), pp. 465–481. DOI: 10.1007/s00170-015-7077-3.

4. Das S., Bourell D.L., Babu S.S. Metallic materials for 3D printing. *MRS Bulletin*, 2016, vol. 41 (10), pp. 729–741. DOI: 10.1557/mrs.2016.217.

5. Cunningham C.R., Flynn J.M., Shokrani A., Dhokia V., Newman S.T. Invited review article: Strategies and processes for high quality wire arc additive manufacturing. *Additive Manufacturing*, 2018, vol. 22, pp. 672–686. DOI: 10.1016/j.addma.2018.06.020.

6. Jin W., Zhang C., Jin S., Tian Y., Wellmann D., Liu W. Wire arc additive manufacturing of stainless steels: a review. *Applied Sciences*, 2020, vol. 10 (5), p. 1563. DOI: 10.3390/app10051563.

7. Li Y., Su C., Zhu J. Comprehensive review of wire arc additive manufacturing: Hardware system, physical process, monitoring, property characterization, application and future prospects. *Results in Engineering*, 2022, vol. 13, p. 100330. DOI: 10.1016/j.rineng.2021.100330.

8. Pattanayak S., Sahoo S.K. Gas metal arc welding based additive manufacturing – a review. *CIRP Journal of Manufacturing Science and Technology*, 2021, vol. 33, pp. 398–442. DOI: 10.1016/j.cirpj.2021.04.010.

9. Kokare S., Oliveira J.P., Santos T.G., Godina R. Environmental and economic assessment of a steel wall fabricated by wire-based directed energy deposition. *Additive Manufacturing*, 2023, vol. 61, p. 103316. DOI: 10.1016/j.addma.2022.103316.

10. Abdulaziz A. A brief review on the common defects in wire arc additive manufacturing. *International Journal of Current Science Research and Review*, 2022, vol. 5 (12), pp. 4556–4576. DOI: 10.47191/ijcsrr/V5-i12-19.

11. Jiamin S., Jonas H., Markus K., Klaus D. Residual stress in wire and arc additively manufactured aluminum components. *Journal of Manufacturing Processes*, 2021, vol. 65, pp. 97–111. DOI: 10.1016/j.jmapro.2021.02.021.

12. Busachi A., Erkoyuncu J., Colegrove P., Martina F., Ding J. Designing a WAAM based manufacturing system for defence applications. *Procedia CIRP*, 2015, vol. 37, pp. 48–53. DOI: 10.1016/j.procir.2015.08.085.

13. Zakir F., Syed A.K., Zhang X., Davis A.E., Sahu V.K., Caballero A.E., Biswal R., Prangnell P.B., Williams S. Microstructure tailoring of a wire-arc DED processed Ti6242 alloy for high damage tolerance performance. *Additive Manufacturing*, 2025, vol. 105, p. 104785. DOI: 10.1016/j.addma.2025.104785.

14. Wang X., Xu L., Zhao L., Han Y. A solution for estimating high-temperature strength based on additive manufacturing characteristics. *International Journal of Mechanical Sciences*, 2023, vol. 245, p. 108124. DOI: 10.1016/j.ijmecsci.2023.108124.

15. Duarte V.R., Rodrigues T.A., Schell N., Miranda R.M., Oliveira J.P., Santos T.G. Hot forging wire and arc additive manufacturing (HF-WAAM). *Additive Manufacturing*, 2020, vol. 35, p. 101193. DOI: 10.1016/j.addma.2020.101193.

16. Elmer J.W., Fisher K., Gibbs G., Sengthay J., Urabe D. Post-build thermomechanical processing of wire arc additively manufactured stainless steel for improved mechanical properties and reduction of crystallographic texture. *Additive Manufacturing*, 2022, vol. 50, p. 102573. DOI: 10.1016/j.addma.2021.102573.

17. McAndrew A.R., Rosales M.A., Colegrove P.A., Hönnige J.R., Ho A., Fayolle R., Eyitayo K., Stan I., Sukrongpang P., Crochemore A., Pinter Z. Interpass rolling of Ti-6Al-4V wire + arc additively manufactured features for microstructural refinement. *Additive Manufacturing*, 2018, vol. 21, pp. 340–349. DOI: 10.1016/j.addma.2018.03.006.

18. Hönnige J.R., Colegrove P., Williams S. Improvement of microstructure and mechanical properties in wire + arc additively manufactured Ti-6Al-4V with machine hammer peening. *Procedia Engineering*, 2017, vol. 216, pp. 8–17. DOI: 10.1016/j.proeng.2018.02.083.

19. Colegrove P.A., Donoghue J., Martina F., Gu J., Prangnell P., Hönnige J. Application of bulk deformation methods for microstructural and material property improvement and residual stress and distortion control in additively manufactured components. *Scripta Materialia*, 2017, vol. 135, pp. 111–118. DOI: 10.1016/j.scriptamat.2016.10.031.

20. Gu J., Ding J., Williams S.W., Gu H., Bai J., Zhai Y., Ma P. The strengthening effect of inter-layer cold working and post-deposition heat treatment on the additively manufactured Al–6.3Cu alloy. *Materials Science and Engineering: A*, 2016, vol. 651, pp. 18–26. DOI: 10.1016/j.msea.2015.10.101.

21. Sun R., Li L., Zhu Y., Guo W., Peng P., Cong B., Sun J., Che Z., Li B., Guo C., Liu L. Microstructure, residual stress and tensile properties control of wire-arc additive manufactured 2319 aluminum alloy with laser shock peening. *Journal of Alloys and Compounds*, 2018, vol. 747, pp. 255–265. DOI: 10.1016/j.jallcom.2018.02.353.

22. Liu J., Ye C., Dong Y. Recent development of thermally assisted surface hardening techniques: A review. *Advances in Industrial and Manufacturing Engineering*, 2021, vol. 2, p. 100006. DOI: 10.1016/j.aime.2020.100006.

23. Thomas M., Jackson M. The role of temperature and alloy chemistry on subsurface deformation mechanisms during shot peening of titanium alloys. *Scripta Materialia*, 2012, vol. 66 (12), pp. 1065–1068. DOI: 10.1016/j.scriptamat.2012.02.049.

24. Harada Y., Mori K. Effect of processing temperature on warm shot peening of spring steel. *Journal of Materials Processing Technology*, 2005, vol. 162–163, pp. 498–503. DOI: 10.1016/j.jmatprotec.2005.02.095.

25. Chen H., Zhou J., Sheng J., Meng X.K., Huang S., Xie X. Effects of warm laser peening on thermal stability and high temperature mechanical properties of A356 alloy. *Metals*, 2016, vol. 6 (6), p. 126. DOI: 10.3390/met6060126.

26. Wang Z., Liu Z., Gao C., Wong K., Ye S., Xiao Z. Modified wear behavior of selective laser melted Ti6Al4V alloy by direct current assisted ultrasonic surface rolling process. *Surface and Coatings Technology*, 2020, vol. 381, p. 125122. DOI: 10.1016/j.surfcoat.2019.125122.

27. Amanov A., Umarov R. The effects of ultrasonic nanocrystal surface modification temperature on the mechanical properties and fretting wear resistance of Inconel 690 alloy. *Applied Surface Science*, 2018, vol. 441, pp. 515–529. DOI: 10.1016/j.apsusc.2018.01.293.

28. Kartashev M.F., Permyakov G.L., Trushnikov D.N., Mindibaev M.R. Issledovanie vliyaniya deformatsionnogo uprochneniya na mekhanicheskie svoistva obraztsov iz splava AMg5, poluchennykh sposobom mnogosloinoi naplavki [Understanding the effect of work hardening on the mechanical properties of aluminum alloy 5056 specimens produced by multilayer surfacing]. *Vestnik Magnitogorskogo gosudarstvennogo tekhnicheskogo universiteta im. G.I. Nosova = Vestnik of Nosov Magnitogorsk State Technical University*, 2019, vol. 17, no. 3, pp. 38–45. DOI: 10.18503/1995-2732-2019-17-3-38-45.

29. Kirichek A.V., Soloviev D.L., Altuhov A.Yu. Deformation wave hardening of metallic materials. *Journal of Nano and Electronic Physics*, 2014, vol. 6 (3), p. 03069.

30. Kirichek A.V., Solovyev D.L., Silantiev S.A., Yashin A.V., Zhidkov M.E. Issledovaniya kombinirovannogo uprochneniya volnovym deformatsionnym vozdeistviem i termoobrabotkoi stali 30KhGSA [Studies of combined hardening by wave deformation action and heat treatment of steel 30KhGSA l]. *Uprochnyayushchie tekhnologii i pokrytiya = Strengthening Technologies and Coatings*, 2022, vol. 18, no. 11 (215), pp. 524–528. DOI: 10.36652/1813-1336-2022-18-11-524-528.

31. Kirichek A.V., Solov'ev D.L. Creating heterogeneous surface structures by static-pulsed treatment. *Russian Engineering Research*, 2008, vol. 28 (3), pp. 277–279. DOI: 10.3103/S1068798X08030209.

32. Belyaev G.S. Vliyanie nagreva na tverdost' i strukturu uprochnennogo sloya [Effect of heating on the hardness and structure of the hardened surface layer]. *Metallovedenie i termicheskaya obrabotka metallov = Metal Science and Heat Treatment*, 1979, no. 11, p. 64. (In Russian).

33. Amininejad A., Jamaati R., Hosseinipour S.J. Influence of deformation and post-annealing treatment on the microstructure and mechanical properties of austenitic stainless steel. *Transactions of the Indian Institute of Metals*, 2021, vol. 74 (7), pp. 1799–1807. DOI: 10.1007/s12666-021-02277-8.

34. Boroumand K., Hadi M., Vafaei R. Hot deformation behavior and constitutive modelling of a medium-carbon structural steel. *Physics of Metals and Metallography*, 2021, vol. 122, pp. 1611–1620. DOI: 10.1134/S0031918X21140052.

35. Kapustova M., Tittel V. Issledovanie vliyaniya temperatury nagreva na mekhanicheskie svoistva i deformiruemost' stali tipa 18KhG pri nepolnoi goryachei deformatsii [Investigation of the influence of heating temperature on the mechanical properties and deformability of 18KhG type steel under incomplete hot deformation]. *Lit'e i metallurgiya = Foundry Production and Metallurgy*, 2006, no. 1 (37), pp. 139–142.

36. Pickering F.B. *Physical metallurgy and the design of steels*. London, Applied Science Publishers, 1978. 275 p. (Russ. ed.: Pikering F.B. *Fizicheskoe metallovedenie i razrabotka stalei*. Moscow, Metallurgiya Publ., 1982. 184 p.).

37. Obitov N., Ruzibaev A. Heat treatment of non-hardened aluminum alloys. *AIP Conference Proceedings*, 2023, vol. 2612, p. 040004. DOI: 10.1063/5.0127487.

38. Shuro I., Umemoto M., Todaka Y., Yokoyama S. Phase transformation and annealing behavior of SUS 304 austenitic stainless steel deformed by high pressure torsion. *Materials Science Forum*, 2010, vol. 654–656, pp. 334–337. DOI: 10.4028/www.scientific.net/MSF.654-656.334.

Conflicts of Interest

The authors declare no conflict of interest.